ORIGINAL ARTICLE

Geochemical characterization of groundwater from an arid region in India

Tirumalesh Keesari · U. P. Kulkarni · Archana Deodhar ·
P. S. Ramanjaneyulu · A. K. Sanjukta ·
U. Saravana Kumar

Abstract A study on the geochemical processes in arid region of western India (Kachchh district) was carried out using major, minor, trace metal data and isotopic composition (δ^2H, δ^{18}O) of groundwaters. Results indicate that the distribution of chemical species in groundwater of this district is controlled by leaching of marine sediments, dissolution of salts in root zone and incongruent dissolution of carbonate minerals. Common inorganic contaminants such as fluoride, nitrate and phosphate are within drinking water permissible limits. However, most of the samples analyzed contain total dissolved salts more than desirable limits and fall in doubtful to unsuitable category with regard to irrigational purpose. Trace metal data indicates no contamination from toxic elements such as arsenic and lead. An increased salt content is observed in groundwater at shallower depths indicating mixing with surface water sources. The chemical characteristics of the groundwater have found to be strongly dependent on the local lithological composition. Environmental isotopic data indicates that the groundwater is of meteoric origin and has undergone limited modification before its recharge. The processes responsible for observed brackishness are identified using chemical and isotope indicators, which are in agreement with subsurface lithology and hydrochemistry. These data though represent hydrochemical scenario of 2001 can still be used for understanding the long-term fluctuations in water chemistry and would be quite useful for the planners in validating groundwater quality models.

Keywords Environmental isotopes · Hydrochemistry · Leaching · Evaporative enrichment · Incongruent dissolution · Kachchh

T. Keesari (✉) · U. P. Kulkarni · A. Deodhar ·
U. Saravana Kumar
Isotope Applications & Radiopharmaceuticals Division, Bhabha
Atomic Research Centre, Mumbai 400 085, India
e-mail: tiruh2o@gmail.com

U. P. Kulkarni
e-mail: upk_51@rediffmail.com

A. Deodhar
e-mail: adeodhar@barc.gov.in

U. Saravana Kumar
e-mail: vsk@barc.gov.in

P. S. Ramanjaneyulu
Radioanalytical Chemistry Division, Bhabha Atomic Research
Centre, Mumbai 400 085, India
e-mail: psr@barc.gov.in

A. K. Sanjukta
Analytical Chemistry Division, Bhabha Atomic Research
Centre, Mumbai 400 085, India
e-mail: sanjuktaak@barc.gov.in

Introduction

Groundwater is an important source of water for human consumption, agricultural and industrial use. In arid and the semi-arid regions, where the rainfall is less than the human consumption, often groundwater becomes the only alternate source of fresh water or may be the most economically viable water supply. Thus, identifying the source and origin of groundwater, and understanding the geochemical processes affecting groundwater quality are crucial for the sustainable water supply in these regions. Hydrochemical and environmental isotopic tools have been found to be very useful in assessing critical hydrological aspects such as groundwater recharge and its dynamics, groundwater quality, etc. (Glynn and Plummer 2005; Edmunds 2009; Herczeg and Leaney 2011).

Kachchh, the largest district of India, is also one of the most water scarce regions. The per capita fresh water availability has reached as low as 414 m³/a in this state (Gupta and Deshpande 2004), while 1,700 m³/a is considered as satisfactory and more than 75 % of the water required for agricultural activities is met by groundwater resources. In addition to severe water scarcity, groundwater quality is also found to be brackish in most of the places and unfit for drinking purposes. Groundwater contamination by fluoride, chloride and nitrate has already been reported in and around the study area (CGWB 2009), which could be due to anthropogenic activities like mining and farming (Singh et al. 1996; IWMI-TATA 2005). In addition, there are also reports on the seawater intrusion into the coastal aquifers of Gujarat due to overexploitation of groundwater resources (Desai et al. 1979; Singh et al. 1996).

Studies in western Gujarat were mostly on geologic, tectonic and palaeontologic aspects (Biswas 1987; Merh 1993, 1995; Maurya et al. 2003; Parag 2002; Thakkar et al. 1999). A few studies were also carried out for evaluating the groundwater resources of Kachchh district using hydrochemistry and environmental isotopic tools. Atomic Minerals Directorate for Exploration and Research, India has carried out investigations on hydrochemical aspects of Kachchh district comprising Kachchh mainland and Wagad basin (Pande et al. 1991), since the main interest was uranium exploration, groundwater chemistry was not studied in detail. Isotope studies carried out by Gupta et al. (2005) were focused mostly on the isotopic signatures of precipitation in north Gujarat, India. To the best of our knowledge, there is no comprehensive study carried out on groundwater resources of Kachchh district involving a combination of hydrochemical and isotope approaches, and the governing geochemical processes and factors affecting groundwater quality were not reported.

There is a pressing need to assess groundwater quality for drinking and irrigational purposes and understand the geochemical processes so that proper management protocols can be established to protect the groundwater resources from further deterioration. For the first time, geochemical and isotopic characterization of groundwaters from major basins of Kachchh district, Gujarat are attempted. Processes responsible for variation of chemical facies in different geological units are studied and possible reasons for brackishness/salinity in groundwater are explored.

Location and geology of the study area

Study area forms the north-western part of the western continental margin of India and is situated at the southern edge of the Indus shelf at right angles to the southern Indus fossil rift (Fig. 1a). This area falls between Latitudes 23° and 24°N and Longitudes 69° and 71°E with an area of about 17,000 km², covering most of the Kachchh district of Gujarat state. Kachchh district consists of (a) the Ranns, salt-encrusted wasteland rising only a few meters above sea level, and inundated during monsoon, divided into the Great Rann to the north and Little Rann to the east, (b) the Banni plains between the Great Rann and the rocky mainland, (c) hilly region with island belts of four rocky projections rising above Rann, (d) the Kachchh mainland and (e) the southern coastal plains. The area accessible to habitation is only about 5,000 km² (Singh et al. 1996).

Kachchh district forms an important site of Mesozoic (up to 250 Ma) and Cenozoic (up to 65 Ma) sedimentation in the western margin of India. The main structural features include six major uplifts, namely Pachcham, Khadir, Bela islands, Chorar hills, Wagad basin and Kachchh mainland, which are surrounded by residual depressions, namely the Great Rann and Little Rann of Kachchh (Fig. 1a). Rann of Kachchh is the remnant of an arm of the sea, which formerly connected the Narmada rift with Sind and separated Kachchh from the mainland (Biswas 1987; Krishnan 1949; Merh 1993, 1995; Wadia 1973). These uplifts have been produced by a group of E-W trending faults, which follow the major tectonic trends of the Precambrian basement (up to 4,000 Ma). The generalized stratigraphy of Kachchh mainland, Khadir and Wagad basin is given in Table 1.

Hydrogeology and hydrology

The climate of the study area is arid and average annual rainfall is about 326 mm that is distributed unevenly and varies year to year. About 94 % of the annual rainfall in the district is received mainly during the southwest monsoon between June and September (Singh et al. 1996). Since the soil is generally porous, most of the rainwater is lost either by evaporation or surface run-off. Temperatures are high most of the year, reaching 50 °C in the May and June (Lyès Ferroukhi 1996). The drainage pattern of the Kachchh district is controlled by the lithological and tectonic features along with the influence of sea level changes during the Quaternary period (Karanth 2006). The Central highland forms the main watershed with numerous consequent streams draining the slopes with a radial pattern and pouring their water and sediment load into the Arabian Sea in the west, the Gulf of Kachchh in the south and the Rann in the north (Fig. 1b).

The major sources of fresh groundwater in the district are located under the Bhuj ridge, which is an elevated zone extending from west to east across the center of the district (Lyès Ferroukhi 1996). Bhuj series consists predominantly

Fig. 1 a Location and
geological map of the study area
(redrawn from Baskaran et al.
1989), b sample location map of
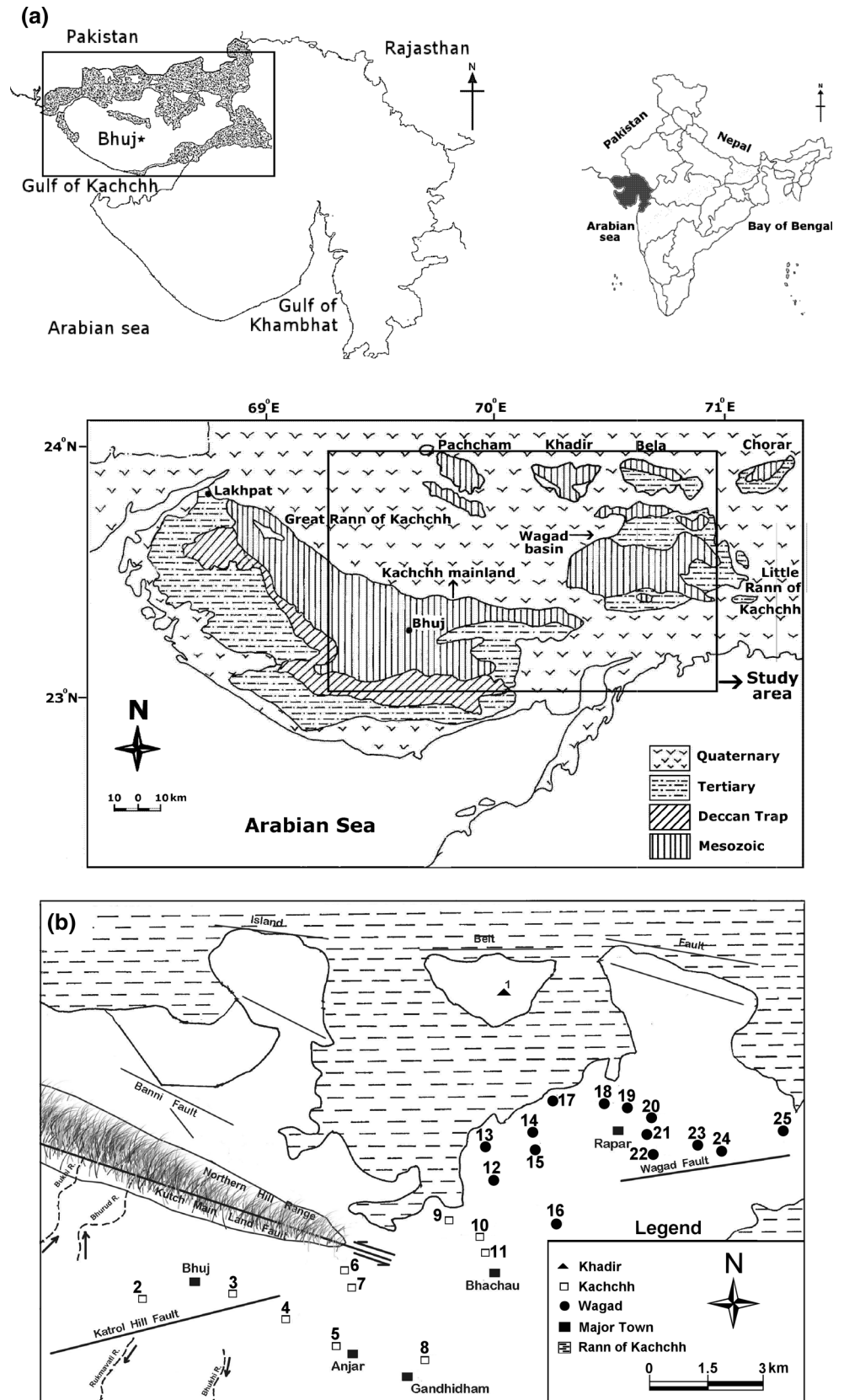the study area. Numbers
correspond to sample ID given
in Table 2

Table 1 Geological stratigraphy of the study area (after Merh 1995)

Period	Time scale	Formation	Lithology	Environment	Water bearing properties (Taylor and Pathak 1960)
Quaternary	Pleistocene–Holocene	Alluvium	Recent deposits, alluvium, Rann silts and blown sands and Miliolite limestone	Estuarine deltaic	Coarse facies yields small to moderate supply of water
Tertiary	Pliocene	Kankawati formation	Upper part pinkish hard calcareous grit and conglomerate containing foraminifers. Gray micaceous and calcareous sandstone	Beach and deltaic	Yields meager to small supply of water
	Early Miocene	Khari formation	Variegated siltstone, grey and khaki clays with fossiliferous marls and contain fossils-like foraminifera and ostracoda	Epineritic to neritic	
Cretaceous	Neocomian–Santonian	Bhuj formation 400–900 m	Upper part: coarse grained feldspathic sandstone, pale brown to dirty white friable, current bedded. Lower part: brown and reddish sandstone with alteration of kaolinitic shale and sandy shale. Shale occasionally carbonaceous and contain plant fossils	Fluviatile to deltaic	Upper Bhuj formation-yields moderate to abundant supply of water

Lower Bhuj formation-yields moderate supply of water |
| | Bathonian–Oxfordian | Washtawa formation (225 m +) | Exposed in central Wagad and consists of shale and sandstone alteration | Littoral to Infralittoral

Upper part in western Wagad and entire Eastern Wagad are Fluviatile to deltaic | |
| | Argovian–(?)Albian | Wagad sandstone (400 m +) | Western part: upper part-brown current bedded sandstone. Lower part: shale and sandstone with marine fossils

Eastern part: brown and red feldspathic sandstone with shale beds and hard purple and black ironstone bands | Lower part in West Wagad is marine sub-littoral. | |
| | Bathonian–Oxfordian | Khadir formation (550 m +) | Upper part: mostly shale with minor sandstone interbeds. Upper middle part: sandstone with thin shale beds. Lower middle part: massive sandstone and shale. Basal part: Grey arkose with wedges of granite cobble conglomerate | Littoral to Infralittoral | |

of current bedded friable sandstones at the top passing downward into alternating sandstones and shales (Merh 1995; Karanth 2006). The upper part of the Bhuj series contains most productive water bearing formations in this region, but the lower part of the series also contains several aquifers, which are less productive. The Laterite is not water bearing but the Deccan trap and the semi-consolidated sandstones have limited potential. In basalt-dominated regions, the zones of weathering between successive lava flows act as aquifers. Along the channels of the larger ephemeral streams of the region, the sand and gravel are water bearing zones and yield small supplies of brackish water to shallow wells. General water table in these areas varies from 4 to 10 m below ground level and slopes towards east (Taylor and Pathak 1960).

Sampling and measurements

A total of 25 water samples from dug wells [depth 15–40 m below ground level (bgl)] and tube wells (depth 75–170 m bgl) were collected from Khadir island, Kachchh mainland and Wagad basin during February 2001 (Fig. 1b). Representative samples were collected by pumping the wells, about 4–5 bore volumes, until a stable temperature in the pumped water is recorded. Water samples were filtered using 0.45 μm pore size membrane filters and stored in polyethylene bottles that were initially washed with 2 % HNO_3 and rinsed with distilled water. Another set was collected and acidified to pH < 2 by adding ultra pure concentrated HNO_3 for cation measurements. Physicochemical parameters such as pH, temperature and electrical conductivity were measured in situ using portable pH/temperature meter (Corning) and conductivity meter (Orion), respectively. Alkalinity was measured in the field by titration method (Table 2). Anions, viz., Cl^-, NO_3^-, F^-, Br^-, PO_4^{3-} and SO_4^{2-} and cations, Na^+, Ca^{2+}, Mg^{2+}, K^+, Li^+ and Sr^{2+} were analyzed using ion chromatography (Dionex) employing electrochemical detector (ED 40) in conductivity mode and boron by spectrophotometer (Table 3). Trace elements like Fe, Al, Mn, Co, Ni, Cu, Zn, As, Cs, Ba and Pb were measured by ICP-MS (Table 4). The charge balance error (CBE) of the chemical data was within ±5 %. For environmental isotopic [deuterium (δ^2H) and oxygen-18 ($\delta^{18}O$)] analyses, representative water samples were collected in 60 mL polyethylene bottles after pumping out the stagnant water. The sample bottles were filled completely and preserved airtight to avoid fractionation due to evaporation. Deuterium and oxygen-18 were measured by mass spectrometer (Geo 20-20, Europa) using gas equilibration method with a precision of ±0.5 and ±0.1 ‰ (2σ criterion), respectively. Stable isotope results were expressed with respect to VSMOW (Vienna Standard Mean Ocean Water) in δ units (‰), where

$$\delta^2H \text{ or } \delta^2O\,(‰) = \frac{R_{sample} - R_{standard}}{R_{standard}} \times 1,000 \qquad (1)$$

and $R = \dfrac{^2H}{^1H}$ or $\dfrac{^{18}O}{^{16}O}$

The stable isotope analysis data are given in Table 5. Saturation indices for Fluorite (CaF_2), Calcite ($CaCO_3$), Gypsum ($CaSO_4$), log P_{CO2} were calculated using NETPATH program (Plummer et al. 1994) and given in Table 5 along with calculated Permeability Index (P.I.), total hardness (T.H.), sodium adsorption ratio (SAR) and sodium percent (Na%).

Results and discussion

Groundwater quality

Basic water quality

Based on the TDS classification by Davis and De Wiest (Davis 1996; Table 6), it is found that the general groundwater quality in Kachchh mainland is fresh to slightly saline in nature (TDS 550–4,000 mg/L) except at one location (no. 8, TDS 8,262 mg/L) and mostly brackish in Wagad basin and Khadir island (TDS 1,500–5,500 mg/L). The dug well samples from both Kachchh mainland (no. 8) and Wagad basin (no. 18) tapping Quaternary formation are found to be saline (TDS > 7,500 mg/L), whereas fresh quality is encountered at a few locations in Wagad basin (nos. 13, 17, 23). The variation in electrical conductivity with respect to depth is depicted in Fig. 2. Groundwater samples belonging to Kachchh mainland (except nos. 8 and 9) show a decreasing trend in electrical conductivity with depth. Group (a) samples belonging to upper Cretaceous sandstone formation are fresh, whereas Group (b) samples tapping Quaternary formation of Wagad basin and Kachchh mainland are saline. The salinity in Quaternary formations could be due to evaporitic enrichment, which is supported by isotopic signatures ("Isotope study"). The data points are more scattered in the case of groundwaters from Wagad basin, which could be due to diverse nature of sediments as demonstrated in stratigraphy (Table 1). Most of the groundwaters show pH between 6.5 and 8.5 while a few samples are slightly acidic (pH 6.2–6.5). Groundwater temperatures are between 28.9 and 32.9 °C. The temperature of shallow groundwater is equal to the mean air temperature above the land surface. Since this district experiences very high temperature up to 50 °C ("Hydrogeology and hydrology"), groundwater temperatures at a few shallow locations reach 32.9 °C.

Table 2 Details of geological formation and physicochemical parameters of the groundwaters, Kachchh district

Location no.	Field id	Location	Formation	Source	Well depth (m, bgl)	Temperature (°C)	pH	EC (μS/cm)	Field alkalinity (mg CaCO$_3$/L)
1	Kh-3	Ratanpar	Khadir	TW	90	31.9	7.3	6,270	385
2	KML-5	Mankuva	Bhuj Sandstone	TW	150	29.7	6.8	1,919	196
3	KML-6	Bhujodi Patia (Kukma)	Tertiary	TW	114	30.4	7.0	2,330	184
4	KML-7	Jap (Ratnal)	Bhuj Sandstone	TW	120	30.5	7.5	1,107	249
5	KML-27	Anjar	Bhuj Sandstone	TW	167	31.4	7.3	784	170
6	KML-26	Chandrani (Bhuj road)	Tertiary	TW	106	32.2	7.0	2,598	245
7	KML-14	Chandrani (Ramdev Pir)	Tertiary	TW	103	31.9	7.0	2,760	251
8	KML-13	Mithi road (Gandhidham)	Quaternary	DW	40	30.1	7.0	12,120	300
9	KML-15	Kabarau (Koyaliwadi)	Tertiary	TW	120	30.2	6.9	5,930	281
10	KML-16	Vondh	Tertiary	TW	76	32.6	6.8	6,930	190
11	KML-17	Bhachau	Tertiary	TW	90	31.7	7.2	4,630	199
12	W-8	Kharoi	Wagad Sandstone	TW	167	30.1	7.3	2,730	263
13	W-9	Kaker (Chaubari)	Wagad Sandstone	TW	127	31.5	7.3	1,364	188
14	W-10	Kharewadi (Ram Vav)	Wagad Sandstone	TW	120	31.5	7.0	3,540	326
15	W-25	Kankoi	Wagad Sandstone	TW	90	29.6	6.8	6,223	380
16	W-24	Adhoi (south)	Tertiary	TW	120	30.5	7.5	5,558	460
17	W-11	Jesada (east)	Wagad Sandstone	DW	27	29.0	7.2	1,576	208
18	W-4	Nandasar (south)	Quaternary	DW	18	28.9	7.2	10,470	350
19	W-12	Rapar-Suvai Road	Wagad Sandstone	TW	155	29.7	6.6	7,680	321
20	W-18	Rapar-Sai Road	Wagad Sandstone	TW	90	30.7	7.0	3,410	267
21	W-19	Sai	Wagad Sandstone	TW	106	32.9	6.3	7,543	252
22	W-20	Lilpar	Wagad Sandstone	TW	100	32.5	6.2	2,541	126
23	W-21	Vallabhpar	Wagad Sandstone	DW	33	31.0	7.2	1,544	232
24	W-22	Padampar	Wagad Sandstone	TW	150	32.3	6.6	4,802	312
25	W-23	Bhangera (Adesar)	Wagad Sandstone	TW	97	30.9	6.2	3,011	166

EC electrical conductivity, *DW* dug well, *TW* tube well

Fluoride, nitrate and phosphate

Fluoride levels in groundwaters of Kachchh mainland and Khadir island vary from 0.4 to 1.4 mg/L and are within acceptable level of 1.5 mg/L (WHO 2008; BIS 2004), whereas in Wagad basin fluoride concentration varies from 0.6 to 2.7 mg/L and it is also within permissible limits in most of the samples. A few samples from Wagad basin (nos. 12, 19, 20, 21 and 24) show relatively high fluoride content (1.7–2.7 mg/L). Very high fluoride concentration of 5.4 mg/L is observed in one sample (no. 8) tapping Quaternary formation of Kachchh mainland. The reason for high F$^-$ could be due to evaporite dissolution from the unsaturated zone, which is evident from its high Cl$^-$ (4,059 mg/L) and presence of significant amount of Br$^-$ (13 mg/L). Nitrate concentration in groundwaters of all locations is within permissible limit of 45 mg/L (WHO 2008; BIS 2004) except at sample nos. 3 and 16 (82 and 60 mg/L). These locations also show comparatively high

phosphate values (6.7 and 1.2 mg/L) indicating contribution of anthropogenic inputs mainly from agriculture.

Trace metals

Among trace metals analyzed, only Ba^{2+} shows higher values and rest of the elements are within natural limits, still the values are within permissible limit for drinking water, i.e. 700 ppb for Ba^{2+} (WHO 2008). Presence of high Ba^{2+} could be due to the occurrence of Shales in the formation (Hitchon et al. 1999). Toxic metals such as arsenic and lead are found to be in the range of 1.3–6.8 ppb and 0.1–7.2 ppb, respectively (Table 4). All the trace elemental concentrations are within drinking water permissible limits set by WHO (2008) excepting two samples (nos. 21 and 25) in the case of Mn^{2+}. This indicates no significant contribution from industrial wastes or it could also suggest no significant geological input to the groundwater system.

Table 3 Major and minor ion data of groundwater

Location no.	Field ID	F⁻ (mg/L)	Cl⁻ (mg/L)	SO₄²⁻ (mg/L)	NO₃⁻ (mg/L)	PO₄³⁻ (mg/L)	HCO₃⁻ (mg/L)	Li⁺ (mg/L)	Na⁺ (mg/L)	K⁺ (mg/L)	Mg²⁺ (mg/L)	Ca²⁺ (mg/L)	Sr²⁺ (mg/L)	Br⁻ (mg/L)	B (mg/L)	Fe (mg/L)	TDS calc. (mg/L)	CBE (%)	Water type
1	Kh-3	1.3	1,678	632	2.0	BDL	470	0.30	1,133	21	154	101	4.0	10	ND	0.08	3,875	−0.3	Na–Cl
2	KML-5	0.8	343	180	10	BDL	269	0.03	268	5.8	35	102	1.7	BDL	ND	0.15	1,074	4.8	Na–Ca–Cl–HCO₃
3	KML-6	1.0	424	200	82	6.7	255	0.06	314	6.2	42	129	3.2	BDL	ND	0.19	1,457	4.8	Na–Ca–Cl
4	KML-7	1.4	148	41	30	BDL	304	BDL	146	1.8	20	67	1.4	BDL	ND	0.19	581	3.9	Na–Ca–HCO₃–Cl
5	KML-27	0.6	116	35	23	BDL	215	BDL	78	3.7	19.7	63	ND	BDL	ND	0.06	556	2.3	Na–Ca–HCO₃–Cl
6	KML-26	0.8	587	172	17	BDL	290	BDL	347	10	60	120	3.2	BDL	ND	0.12	1,610	2.3	Na–Ca–Cl
7	KML-14	0.6	750	162	12	BDL	306	0.01	455	7.2	62	105	4.5	3.0	0.8	0.06	1,968	1	Na–Cl
8	KML-13	5.4	4,059	646	45	BDL	366	0.20	2,560	10	230	306	23.9	13	2.2	BDL	8,262	4.1	Na–Cl
9	KML-15	1.0	1,610	400	38	BDL	343	0.14	1,018	16	92	243	5.8	BDL	1.0	BDL	3,773	4.7	Na–Cl
10	KML-16	1.0	1,840	405	BDL	BDL	250	0.05	1,078	15.4	96.5	302	2.5	BDL	0.6	BDL	3,995	4.5	Na–Ca–Cl
11	KML-17	0.4	1,160	246	36	BDL	365	BDL	806	9.2	67.5	143	2.6	1.3	ND	BDL	2,837	3.9	Na–Cl
12	W-8	1.7	519	204	29	BDL	321	0.04	386	3.1	52	106	2.0	ND	ND	BDL	1,624	3.6	Na–Ca–Cl–HCO₃
13	W-9	0.6	256	94	11	BDL	229	0.02	151	4.7	17.0	120	1.0	BDL	0.3	BDL	885	3.6	Na–Ca–Cl–HCO₃
14	W-10	1.4	679	394	BDL	BDL	400	0.10	410	16	79	197	2.2	BDL	ND	0.08	2,181	1.1	Na–Ca–Cl–SO₄
15	W-25	1.0	1,660	644	30	BDL	463	0.20	865	10	144	295	6.1	7.0	1.6	BDL	4,131	−2.7	Na–Ca–Cl–SO₄
16	W-24	1.5	1,388	311	60	1.2	561	BDL	ND	ND	ND	ND	3.0	ND	ND	0.09	–	–	–
17	W-11	0.8	230	194	24	BDL	256	0.02	185	11	43	91	1.6	BDL	ND	0.06	902	4.2	Na–Ca–Cl–HCO₃
18	W-4	1.1	2,490	1,875	33	BDL	427	0.20	1,800	48	338	424	4.9	BDL	1.9	0.07	7,449	4.9	Na–Mg–Cl–SO₄
19	W-12	2.7	1,870	1,560	23	BDL	394	0.22	1,251	22	216	393	4.8	4.0	1.6	BDL	5,498	0.3	Na–Ca–Cl–SO₄
20	W-18	1.9	695	361	23	BDL	327	0.06	525	8.0	56	136	1.6	BDL	ND	BDL	1,924	2.3	Na–Ca–Cl–SO₄
21	W-19	2.4	1,440	1,123	5	BDL	277	BDL	982	14	143	232	2.1	3.5	1.4	1.10	3,949	−1.7	Na–Cl–SO₄
22	W-20	1.4	525	351	14	BDL	155	0.30	390	25	32	107	1.7	3.0	ND	3.90	1,471	1.8	Na–Ca–Cl–SO₄
23	W-21	1.3	239	184	44	BDL	255	BDL	ND	ND	ND	ND	ND	ND	ND	0.16	–	–	–
24	W-22	1.8	1,064	482	22	BDL	381	0.30	709	25	110	140	0.8	5.0	1.2	0.09	2,741	1.1	Na–Cl–SO₄
25	W-23	1.1	690	275	19.4	BDL	203	0.06	410	17.7	37.5	128	0.6	BDL	ND	BDL	1,782	−1.9	Na–Ca–Cl–SO₄
WHO (2008)/BIS (2004)		1.5	250	200	45	–	240	–	–	–	30	75	–	–	0.5	0.3			
% of samples exceeding limits		24	84	72	12	–	84	–	–	–	88	92	–	–	36	8			

Detection limits for NO₃⁻ (0.5 mg/L), PO₃³⁻ (1 mg/L), Li⁺ (0.01 mg/L), Br⁻ (0.5 mg/L), Fe (0.01 mg/L)

CBE charge balance error, ND not determined, BDL below detection limits, Kh Khadir island, KML Kachchh mainland, W Wagad basin

Table 4 Trace metal ion data of groundwaters

Location no.	Field ID	Al (μg/L)	Mn (μg/L)	Co (μg/L)	Ni (μg/L)	Cu (μg/L)	Zn (μg/L)	As (μg/L)	Cs (μg/L)	Ba (μg/L)	Pb (μg/L)
1	Kh-3	BDL	189	0.85	BDL	5.4	BDL	BDL	6.5	17.5	0.9
2	KML-5	11.3	197	2.9	8.9	2	5.6	2.5	5.5	41.6	1.6
3	KML-6	36.5	81.5	1.9	9.3	4.1	11.8	3.2	5.6	49.7	2.5
4	KML-7	105	4.3	0.5	4.2	5.5	10.2	2.5	5	96.6	3.5
5	KML-27	142	6.8	0.7	4.4	2.1	11.7	2.6	5.2	128	3.3
6	KML-26	417	8.5	1.2	7.6	1.7	10.7	2.9	5.2	162	7.2
7	KML-14	BDL	173	0.8	BDL	BDL	BDL	BDL	2.4	128	2.6
8	KML-13	BDL	2.4	0.2	BDL	BDL	BDL	BDL	5.8	131	1
9	KML-15	5.4	8.6	0.3	0.2	4.6	BDL	BDL	2.4	157	3.4
10	KML-16	BDL	0.8	0.4	BDL	BDL	BDL	BDL	6.5	0	BDL
11	KML-17	82.6	3.8	0.5	1	BDL	BDL	BDL	2.8	37	0.4
12	W-8	BDL	2.3	2.3	10.6	0.9	13.1	3.2	5.1	113	1.2
13	W-9	19.2	10	0.5	5.9	1.2	9.6	2.4	5	122	1.3
14	W-10	29.8	93.2	0.44	0.2	0.4	4.2	BDL	2.6	63.4	2.6
15	W-25	73.3	94	8	20	BDL	12	BDL	6	27.5	0.8
16	W-24	82.4	66.3	0.9	2.3	2.1	5.3	4.7	5.1	119	2
17	W-11	133	40	8.7	15.5	6.8	49.2	1.3	5.2	130	1.3
18	W-4	BDL	59.5	0.42	BDL	BDL	BDL	BDL	6.5	8.5	BDL
19	W-12	BDL	145	1.5	BDL	2.5	BDL	BDL	6	15.1	2
20	W-18	BDL	13.6	0.4	1.5	BDL	6.2	BDL	2.6	32	BDL
21	W-19	BDL	1,041	12.4	18.5	BDL	20.2	BDL	6.5	8	BDL
22	W-20	55.3	322	41.2	120	1.9	65.5	6.8	5.6	83.3	2.6
23	W-21	45.6	57.8	3	11.2	2.6	9.9	2.6	5.3	148	3.6
24	W-22	38.6	80.2	2.6	8	1.6	12	BDL	3	28.4	1.4
25	W-23	13.2	684	6.8	9	0.7	8.2	BDL	3.2	27.9	0.1
WHO (2008)/BIS (2004)		300	100	–	20	50	5,000	10	–	700	10
% of samples exceeding limits		4	28	–	4	Nil	Nil	Nil	–	Nil	Nil

Detection limits in μg/L; Al (5), Ni (0.1), Cu(0.50, Zn(1), As(1), Pb(0.1)

Drinking and irrigational suitability

Higher concentration of TDS decreases the palatability and may cause gastro-intestinal irritation in human and may also have laxative effects. The enrichment of TDS is mainly governed by dissolution of salts and evaporation of water. TDS in groundwaters of this district ranges between 556 and 8,262 mg/L. As per the BIS (2004) classification, TDS value of 500 mg/L is the desirable limit for drinking purpose. All the samples show TDS values above permissible limits. Among different trace elements measured, it is found that mainly Mn^{2+} and B concentrations fall above desirable limits (Tables 3, 4).

Hardness is defined as the sum of concentration of their ions expressed in mg/L of $CaCO_3$. Hardness increases due to metallic ions dissolved in water. The total hardness (T.H.) in groundwaters is found to range from 238 to 2,450 mg $CaCO_3$/L. Total hardness of more than 120 mg

$CaCO_3$/L is considered as very hard water, as per classification by Durfor and Becker (1964). Therefore, all the groundwaters can be classified as very hard.

Irrigation suitability of groundwater is mainly evaluated based on electrical conductivity (EC), sodium adsorption ratio (SAR), percent of sodium (Na%) and Permeability Index (P.I.). These indicators are calculated using the formulae:

$$SAR = \frac{Na^+}{\sqrt{\frac{Ca^{2+} + Mg^{2+}}{2}}} \tag{2}$$

$$Na\% = \frac{(Na^+ + K^+) \times 100}{Ca^{2+} + Mg^{2+} + Na^+ + K^+} \tag{3}$$

$$P.I. = \frac{(Na^+ + HCO_3^-) \times 100}{\sqrt{Ca^{2+} + Mg^{2+} + Na^+}} \tag{4}$$

where the concentrations are reported in meq/L.

Table 5 Saturation indices, SAR, Na% and stable isotope data of groundwaters

Location no.	Field ID	δ^2H (‰ VSMOW)	$\delta^{18}O$ (‰ VSMOW)	d-excess (‰ VSMOW)	SI_fluorite	SI_calcite	SI_gypsum	Log pCO_2	SAR	Na%	T.H.	P.I.
1	Kh-3	−25.60	−5.09	15.12	−1.22	0.17	−1.20	−1.76	16.5	73.6	886	78
2	KML-5	−29.20	−5.33	13.44	−1.28	−0.44	−1.39	−1.52	5.8	59.5	399	70
3	KML-6	−35.20	−5.79	11.12	−1.03	−0.18	−1.30	−1.75	6.1	58.1	495	67
4	KML-7	−28.70	−5.00	11.30	−0.87	0.27	−2.08	−2.09	4.0	56.0	250	76
5	KML-27	−25.30	−4.90	13.90	−1.61	−0.07	−2.13	−2.05	2.2	42.1	238	65
6	KML-26	−45.40	−7.06	11.08	−1.31	−0.08	−1.43	−1.62	6.4	58.2	547	66
7	KML-14	−49.90	−7.27	8.26	−1.64	−0.14	−1.53	−1.51	8.7	65.7	517	73
8	KML-13	−20.00	−3.15	5.20	0.35	0.12	−0.92	−1.62	26.8	76.4	1,711	78
9	KML-15	−29.70	−4.65	7.50	−0.98	0.03	−0.98	−1.50	14.1	69.3	985	73
10	KML-16	−34.20	−4.90	5.00	−0.93	−0.13	−0.92	−1.56	13.8	67.1	1,151	70
11	KML-17	−31.10	−4.86	7.78	−1.93	0.03	−1.31	−1.93	13.9	73.4	635	79
12	W-8	−35.20	−5.18	6.24	−1.06	0.17	−1.39	−1.90	7.6	63.6	479	72
13	W-9	−23.40	−4.25	10.60	−1.41	0.18	−1.54	−2.02	3.4	47.4	370	61
14	W-10	−31.40	−5.00	8.60	−0.69	0.18	−0.96	−1.51	6.2	52.6	817	60
15	W-25	−24.30	−3.83	6.34	−0.95	0.10	−0.75	−1.26	10.3	58.6	1,329	63
16	W-24	−29.80	−5.00	10.20	–	–	–	−1.23	–	–		
17	W-11	−35.80	−5.02	4.36	−1.32	−0.06	−1.39	−1.89	4.0	50.6	404	63
18	W-4	−18.70	−3.23	7.14	−0.95	0.46	−3.62	−1.76	15.8	61.7	2,450	64
19	W-12	−29.50	−4.37	5.46	−0.37	−0.15	−0.38	−1.17	12.5	59.3	1,870	62
20	W-18	−26.80	−5.10	14.00	−0.54	−0.61	−1.12	−1.60	9.5	66.8	570	73
21	W-19	−20.70	−3.23	5.14	−0.32	−0.63	−0.64	−0.93	12.5	64.7	1,168	68
22	W-20	−26.90	−5.23	14.94	−0.87	−1.23	−1.16	−1.10	8.5	68.7	399	74
23	W-21	−25.40	−4.60	11.40	–	–	–	−1.80	–	–	–	–
24	W-22	−33.90	−4.80	4.50	−0.71	−0.41	−1.08	−1.13	10.8	66.1	802	71
25	W-23	−26.20	−4.92	13.16	−0.99	−1.05	−1.20	−0.99	8.2	65.7	474	72

SI Log (IAP/K_sp), *IAP* ion activity product, *Ksp* solubility product, *SAR* sodium absorption ratio (Eq. 2), *Na%* sodium percent (Eq. 3), *P.I.* permeability index (Eq. 4), *T.H.* total hardness

According to Richards (1954), the irrigation water is classified into five groups based on EC as given in Table 7. High EC in water leads to formation of saline soil. It can be found that majority of the samples fall in doubtful to unsuitable category (Table 7). The irrigation water containing high proportions of sodium will enhance the exchange reaction between water and soil for alkaline earth metals, affecting the soil permeability and the texture which makes the soil hard to plough and unsuitable for seedling emergence (Trivedy and Goel 1984). The sodium/alkali hazard is typically expressed as the SAR. This index quantifies the proportion of sodium (Na^+) to calcium (Ca^{2+}) and magnesium (Mg^{2+}) ions in a given water sample (Richards 1954). When the concentration of sodium ion is high in irrigation water, Na^+ tends to be absorbed by clay particles displacing magnesium and calcium ions. This exchange process of Na^+ in water for Ca^{2+} and Mg^{2+} in soil reduces the permeability and eventually results in soil with poor internal drainage (Karanth 1987). SAR varies from 2.2 to 26.8 and majority of samples fall in low sodium

hazard class (Table 7). In addition to SAR, Na% is also a common parameter to assess its suitability for agricultural purposes (Wilcox 1955). Sodium in the presence of inorganic carbon (HCO_3^- and CO_3^{2-}) forms alkaline soils, while it combines with chloride to form saline soils. Both these soils are not favorable for plant growth. A maximum of 60 % of Na% in groundwater is allowed for agricultural purposes (Ramakrishna 1998). Na% in groundwaters of this study area ranges from 42.1 to 76.4 %. It is found that half of the samples fall in permissible class and rest in unsuitable class (Table 7). Presence of high Na% in waters along with high EC reduces the osmotic activity of plants and thus interferes with the absorption of water and nutrients from the soil (Tijani 1994). The combined effect of EC and Na% can be visualized using Wilcox diagram (Wilcox 1955). Figure 3 shows that nearly half of the groundwater samples fall in unsuitable category.

P.I. is an important factor, which influences the quality of irrigation water in relation to soil for development in agriculture (Ragunath 1987; Doneen 1948). Based on P.I.,

Table 6 Water classification based on TDS (Davis and Wiest 1996)

Parameter (range in groundwaters of study area)	Limits	Water class	Number of samples
TDS mg/L (556–8,262)	<1,000	Fresh	4
	1,000–3,000	Brackish	11
	3,000–10,000	Moderately saline	8
	10,000–35,000	Very saline	Nil
	>350,000	Brine	Nil

groundwater is classified into three classes (Domenico and Schwartz 1990), class I (40–60) as good, class II (60–80) as intermediate and class III (80–100) as unsuitable for irrigation, The P.I. in groundwaters ranges from 60 to 79 with an average value of 69, indicating that the water is in intermediate class and suitable for irrigation purposes.

Major ion trends

The major ion data were plotted in Durav diagram (Fig. 4) to find out chemical types and variation in chemical facies. The plot permits the cation and anion compositions of many samples to be represented on a single graph from which major groupings and geochemical trends can be easily discerned. The figure shows five major chemical types, viz., Na–Ca–HCO₃–Cl, Na–Ca–Cl–HCO₃, Na–Ca–Cl–SO₄, Na–Ca–Cl and Na–Cl. Evolution of groundwater from Na–Ca–HCO₃–Cl type [Group (a)] to Na–Ca–Cl–SO₄ type [Group (b)] and finally to Na–Cl [Group (c)] type is clearly discerned from Durav's plot (Fig. 4). Groundwater from Kachchh mainland is found to be Na–Ca–HCO₃–Cl, Na–Ca–Cl–HCO₃, Na–Ca–Cl and Na–Cl types, whereas it is dominantly Na–Ca–Cl–SO₄ type in Wagad basin. Fresh water samples from Wagad basin (nos. 17 and 23) are of Na–Ca–Cl–HCO₃ type. Wells tapping Quaternary formation are of Na–Mg–Cl–SO₄ (no. 18) and Na–Cl (no. 8) chemical types. Even though both the samples tap Quaternary formation with similar salinity, there is a marked difference in their facies. Sample from Wagad basin (no. 18) show high Mg²⁺, Ca²⁺ and SO₄²⁻ concentrations compared to the one from Kachchh mainland (no. 8), which could be due to variation in their lithology (Table 1). This is in agreement with EC variations in Wagad basin ("Basic water quality"). A considerable spatial variation in sediment nature of this district is observed in Holocene stratigraphy by Merh (1993).

The possible sources and processes leading to groundwater brackishness in this area could be dissolution of marine sediments, modern/old seawater intrusion or evaporitic enrichment. In order to identify the source of salinity and understand geochemical processes governing groundwater salinity, major ions data have been plotted against
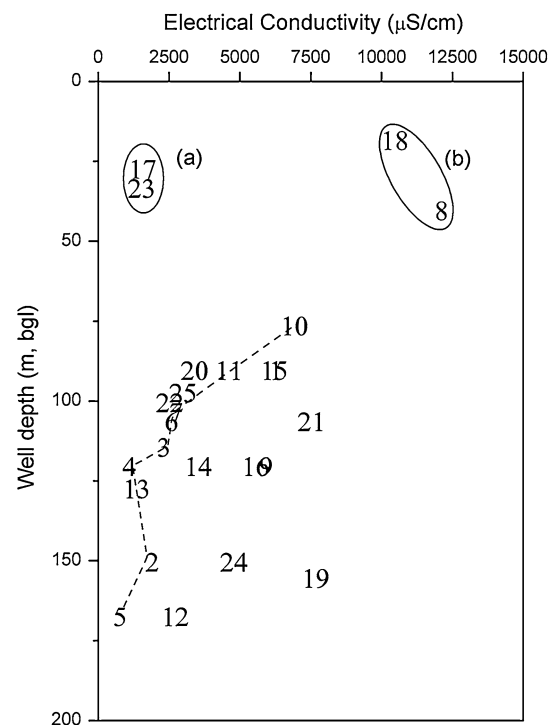
Fig. 2 Plot of electrical conductivity of the water samples versus well depth. *Solid line* is an eye guide to the sample data of Kachchh mainland (except sample nos. 8 and 9). Group (*a*) represents fresh water samples from upper Cretaceous sandstone formation and Group (*b*) represents saline water samples from Quaternary formation of Kachchh and Wagad

chloride with reference to a dilution line representing corresponding seawater ratios (Fig. 5a–f). Chloride and other ion data for seawater were taken from Hitchon et al. (1999) and corresponding ion/chloride ratios were calculated. Data falling on this seawater dilution line indicate seawater component, whereas deviations of the data points away from this line indicate either secondary mixing or chemical/biological reactions such as mineral precipitation/dissolution, ion exchange and sulfate reduction etc.

Sample data fall on the seawater dilution line in the case of sodium vs. chloride plot (Fig. 5a). A high positive correlation observed between Na⁺ and Cl⁻ concentrations indicates a common source for these ions in the groundwater ($R = 0.99$). This illustrates the preservation of more or less the same Na⁺/Cl⁻ ratio in all the groundwater samples, which can be explained by the dominating influence of marine components such as modern/old seawater or evaporates or marine sediments. Concentrations of all ions increase with chloride content (Fig. 5a–e) except for HCO₃⁻ (Fig. 5f) indicating that there are some geochemical processes limiting bicarbonate increase. All the groundwater samples show significant enrichment in Ca²⁺, SO₄²⁻ and HCO₃⁻ concentrations above the reference seawater dilution line (Fig. 5d–f). Since the formations

Table 7 Irrigational suitability of groundwaters

Parameter (range in groundwaters of study area)	Limits	Water class	Number of samples
Na% (Wilcox 1955) (42.1–76.4)	<20	Excellent	Nil
	20–40	Good	Nil
	40–60	Permissible	10
	60–80	Doubtful	13
	>80	Unsuitable	Nil
SAR (Richards 1954) (2.2–26.8)	<10	Excellent	13
	10–18	Good	9
	18–26	Permissible	Nil
	>26	Doubtful	1
EC (Richards 1954) (784–12,120 μS/cm)	<250	Excellent	Nil
	250–750	Good	Nil
	750–2,000	Permissible	6
	2,000–3,000	Doubtful	5
	>3,000	Unsuitable	14
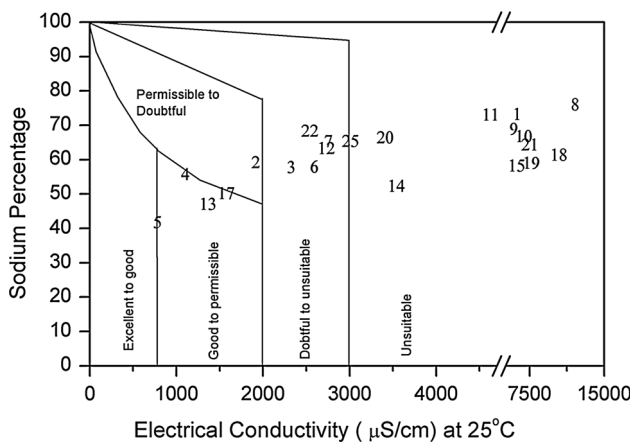
Fig. 3 Wilcox plot of groundwater samples depicting irrigational suitability

Fig. 4 Durav plot of the major ion data of groundwater samples from the study area. The *chemical types* indicate decreasing relative abundance of major ions. Groups *a*, *b* and *c* indicate variation in groundwater facies from fresh [Group *a*] to saline quality [Group *c*]

comprise marine carbonates, gypseous shales, mudstone and feldspathic sandstone, chemical diagenesis might have led to a net addition of these ions from rock to groundwater. Potassium values are found to be scattered on the dilution line (Fig. 5b), but most of the sample data show a fall below seawater dilution line, which could be due to preferential removal of potassium by adsorption on to clay layers. Na^+ and Mg^{2+} concentrations of most of the samples fall slightly above the dilution line (Fig. 5a, c) indicating net addition of these ions from rocks. In order to distinguish between invading and retreating saline water bodies, a plot of Na^+/Cl^- ratio versus chloride concentrations is used (Mercado 1985; Vengosh et al. 1999). Figure 6 shows the plot of Na^+/Cl^- ratio versus Cl^-, in which all the sample data fall above the seawater value of

0.56, excepting sample no. 15. This clearly indicates that the observed brackishness or salinity in the groundwater is not due to present day seawater intrusion, but rather could be due to flushing of saline water or marine sediments that are already present in the aquifer by freshly recharged precipitation. The variability in Na^+/Cl^- ratio can be attributed to variability in cation exchange capacities of the formation.

Earlier study by Pande et al. (1991) in Kachchh and Wagad areas showed that groundwater is fresh to saline in nature (EC; 300–23,000 μS/cm), but there was no discussion on the major ion trends and geochemical processes governing the groundwater chemistry. On the other hand, study by Desai et al. (1979) indicated that salinity in groundwater was due to sea water intrusion, which was deduced from the major ion trends. But, in this study, major ion results and ionic ratios indicate that the seawater intrusion was not the cause for the observed brackishness in groundwater unlike in other regions and it could be due to dissolution of marine sediments or flushing of remnant saline water. This aspect is further confirmed by minor ion trends and stable isotope indicators as discussed in the following sections.

Attempts to distinguish between different saline sources like modern/old seawater, entrapped seawater or dissolution of marine sediments using major ion chemical parameters were found to be inconclusive because these saline sources displayed major ion chemical characteristics that are closely similar to seawater.

Fig. 5 Plot of major ion concentration versus corresponding chloride concentration of the water samples. The *dotted* and *solid lines* represent regression line and ion/chloride ratio of seawater, respectively
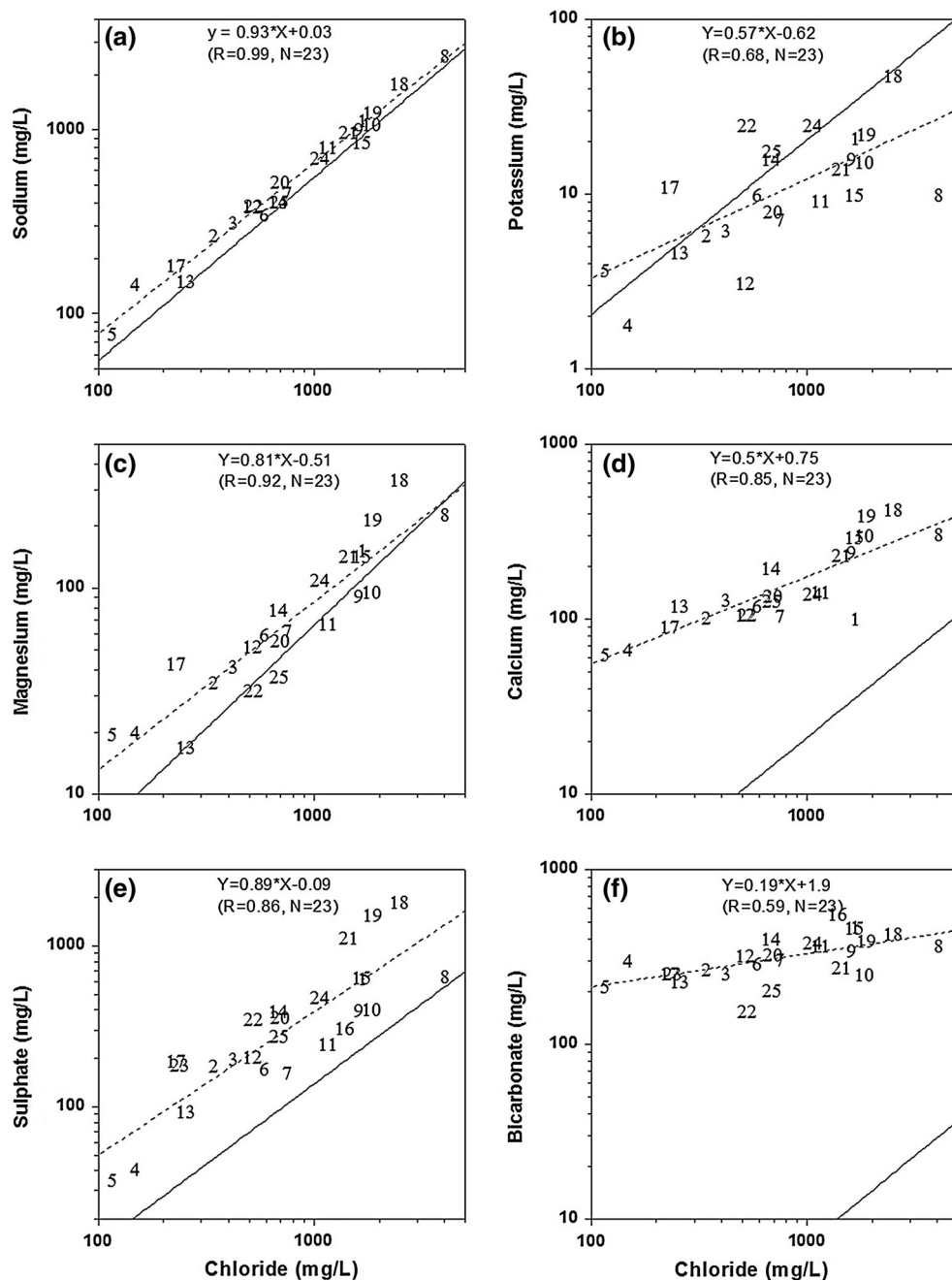
Minor ion trends

Examination of minor ions can help in demarcating different sources of salinity (Elliot et al. 1998). Therefore, in addition to major ions, lithium, strontium, boron and bromide were also determined in these groundwater samples to assess their usefulness as hydrochemical indicator elements for the salinity.

Strontium concentrations in the groundwaters of study area range from 0.6 to 24 mg/L. In most sedimentary aquifers, the strontium levels are primarily controlled by the reaction of groundwater with carbonate or sulfate

minerals present (Hitchon et al. 1999). Dissolution of minerals like aragonite or gypsum, or evaporite deposits or mixing of meteoric water with the interstitial water are the common processes for strontium increase in groundwater (Edmunds et al. 1987). A marked enrichment of strontium is observed in these groundwaters with respect to seawater dilution line (Fig. 7a). This high Sr^{2+} concentration in groundwater could be attributed to recrystallisation of aragonite or dissolution of Gypsum. Aragonite dissolves in water and re-precipitates forming stable calcite form (inversion of crystal structure) releasing Sr^{2+} into groundwater, because Sr^{2+} fits in readily in the
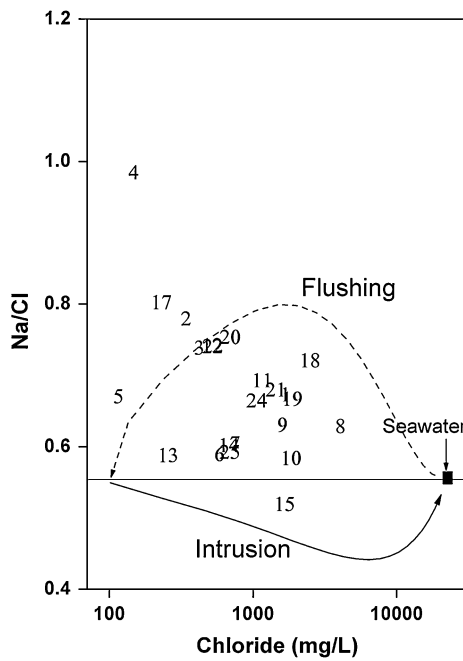
Fig. 6 Plot of Na^+/Cl^- ratio versus chloride concentration of the water samples. *Solid line* indicates Na^+/Cl^- ratio of seawater (0.56), whereas *solid arrow* indicates seawater intrusion and *dashed arrow* indicates flushing trends

orthorhombic aragonite structure but not in rhombohedral calcite structure (Hanshaw and Back 1979). Lithium concentration varies between 0.03 and 0.3 mg/L in groundwater of this district. All the groundwaters show significant enrichment above the reference seawater dilution line (Fig. 7b) indicating leaching of Li^+ from subsurface sediments.

Bromide value of groundwater samples ranges from 1.3 to 13 mg/L. Bromide is considered to be the most conservative ion in evaporating seawater. It continues to concentrate even after halite deposition has commenced (Rittenhouse et al. 1969). Bromide values are found to be scattered on the seawater dilution line (Fig. 7c). Bromide enrichment could be most probably due to degradation of organic matter (Davis 1977), while depletion might occur due to dissolution of halite. Presence of organic matter in the formations of this region is reported by Khadkikar et al. (1999), and also mentioned in the subsurface stratigraphy of this district (Merh 1995; Table 1). Boron concentration in groundwaters varies from 0.3 to 2.2 mg/L. Groundwaters show enrichment in boron content compared to seawater dilution line (Fig. 7d). All these samples are from Wagad basin and Tertiary formation of Kachchh mainland. The presence of clay, kaolinitic shale, micaceous sandstone, etc., in these formations (Table 1) can lead to low permeability and hence sluggish groundwater flows (Karanth 2006; Taylor and Pathak 1960). This condition facilitates greater water–sediment interaction leading to

accumulation of boron in groundwater, which is also evident from brackish quality of these groundwaters.

Carbonate equilibrium

Dolomite $[CaMg(CO_3)_2]$, calcite, Mg-calcite and gypsum are the principal mineral sources for bicarbonate, sulfate, magnesium and calcium present in the subsurface of this district. Relationships between Ca^{2+}, Mg^{2+}, HCO_3^- and SO_4^{2-} can distinguish among different geochemical reactions governing the evolution of the groundwaters pertaining to these ions. The geology of the studied area indicates that the rocks are mainly composed of silicate, carbonate minerals and gypsum (Table 1). As the carbonate minerals in this district are derived from marine sources, impurities like Mg^{2+} or other mineral phases like aragonite cannot be completely ruled out. It is reported that calcite may contain up to 30 % Mg^{2+} (Hanshaw and Back 1979). Petrologic studies conducted in this area have indicated the presence of high Mg-calcite and aragonite in carbonate minerals (Baskaran et al. 1989; Bhatt 2003). To evaluate the geochemical reactions governing Ca^{2+}, Mg^{2+}, HCO_3^- and SO_4^{2-} concentrations in these groundwaters, following reactions were examined.

$$CaMg(CO_3)_2 + H_2O + CO_2 \rightarrow Ca^{2+} + Mg^{2+} + 4HCO_3^-$$
(congruent dissolution of dolomite)

$$CaCO_3 + H_2O + CO_2 \rightarrow Ca^{2+} + 2HCO_3^-$$
(congruent dissolution of calcite)

$$High\ Mg\text{-}calcite \rightarrow Low\ Mg\text{-}calcite + Mg^{2+} + 2HCO_3^-$$
(incongruent dissolution)

$$CaSO_4 \cdot 2H_2O \rightarrow Ca^{2+} + SO_4^{2-} + 2H_2O$$
(dissolution of gypsum)
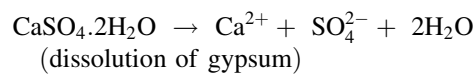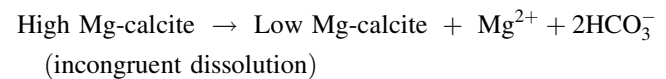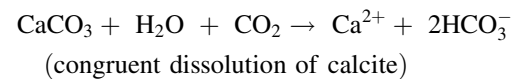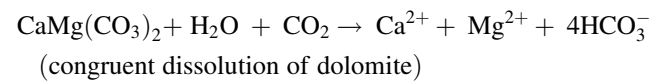
Groundwater samples show a poor correlation between non-gypsum calcium $(Ca^{2+}-SO_4^{2-})$ and bicarbonate (Fig. 8a) and fall below the line representing congruent dissolution of calcite. This shows that calcium concentration in groundwater is less than that would be expected from congruent dissolution of calcite. The depletion in Ca^{2+} concentration could be due to ion exchange or calcite re-precipitation. Since the data points fall above the seawater dilution line in the case of Ca^{2+} vs Cl^- plot (Fig. 5d), it suggests that ion exchange could not be the reason for depletion in Ca^{2+} concentration. On the other hand, these samples are saturated to super saturated with respect to calcite (except no. 25), so calcite re-precipitation could be the governing process for the observed depletion in calcium. The Ca^{2+} and HCO_3^- concentrations in groundwater are controlled by other

Fig. 7 Plot of minor ion concentration versus corresponding chloride concentration of the water samples. The *dotted* and *solid* lines represent regression line and ion/chloride ratio of seawater, respectively
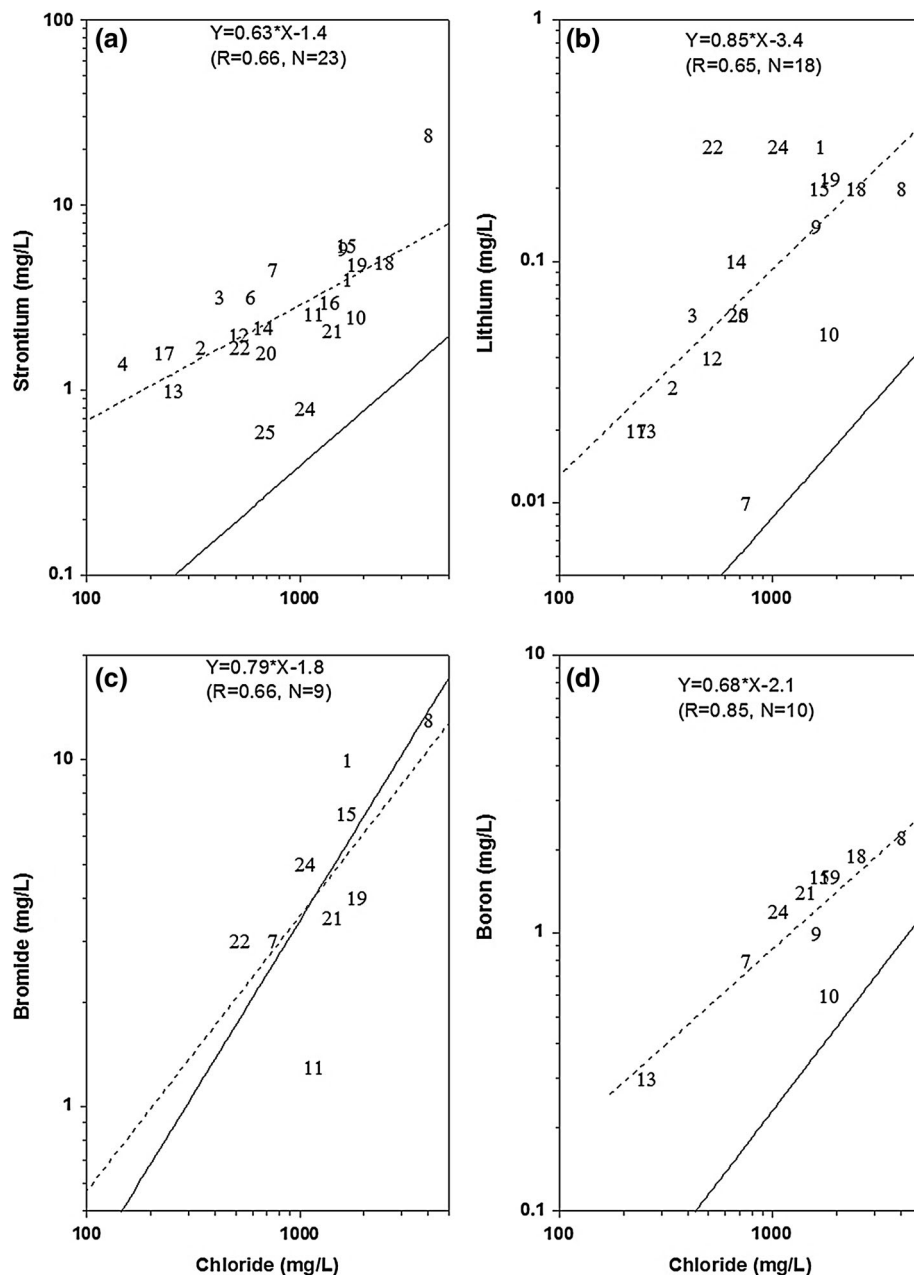
processes in addition to dissolution of calcite. A poor correlation between Ca^{2+} and SO_4^{2-} and HCO_3^- concentrations also reflects the complex geochemical processes involving other minerals present in the aquifer. A few samples show negative Ca^{2+}–SO_4^{2-} values, which could be due to calcite re-precipitation or calcium removal by ion exchange or sulfate addition from other sources. Since these samples have $SI_{calcite}$ less than unity (Table 5), calcite precipitation is not thermodynamically feasible and also sample data fall above seawater–fresh water mixing (sw–fw) line in the plot of Ca^{2+} vs Cl^- (Fig. 5d), implying that ion exchange is not the cause. Sulfate addition from other sources seems to be the most plausible reason.

Groundwater samples show a positive correlation between non-carbonate Ca^{2+} (Ca^{2+}–$0.25*HCO_3^-$) and SO_4^{2-} content with a regression coefficient of 0.77 and the sample data fall very close to the line indicating dissolution of gypsum (Fig. 8b). From the observations noted in Fig. 8a and b, it can be concluded that source of sulfate is gypsum. A few samples (nos. 1, 18, 19, 21 and 24) show deviation from the gypsum dissolution line (fall below the line) and also show negative Ca^{2+}–SO_4^{2-} values in Fig. 8a. Additional source of SO_4^{2-} could be pyrite oxidation. In Mg^{2+} versus HCO_3^- plot (Fig. 8c), sample data fall on regression line with a slope of 0.5 and regression coefficient of 0.94, which represents incongruent

Fig. 8 **a** Plot of non-gypsum calcium versus bicarbonate, *line* indicates congruent dissolution of calcite, **b** plot of non-carbonate calcium versus sulfate, *line* indicates gypsum dissolution, **c** plot of magnesium concentration versus bicarbonate concentration, *solid line* indicates incongruent dissolution of high Mg-calcite, *dotted lines (i and ii)* and *circle* indicates sample data deviating from the *dilution line*
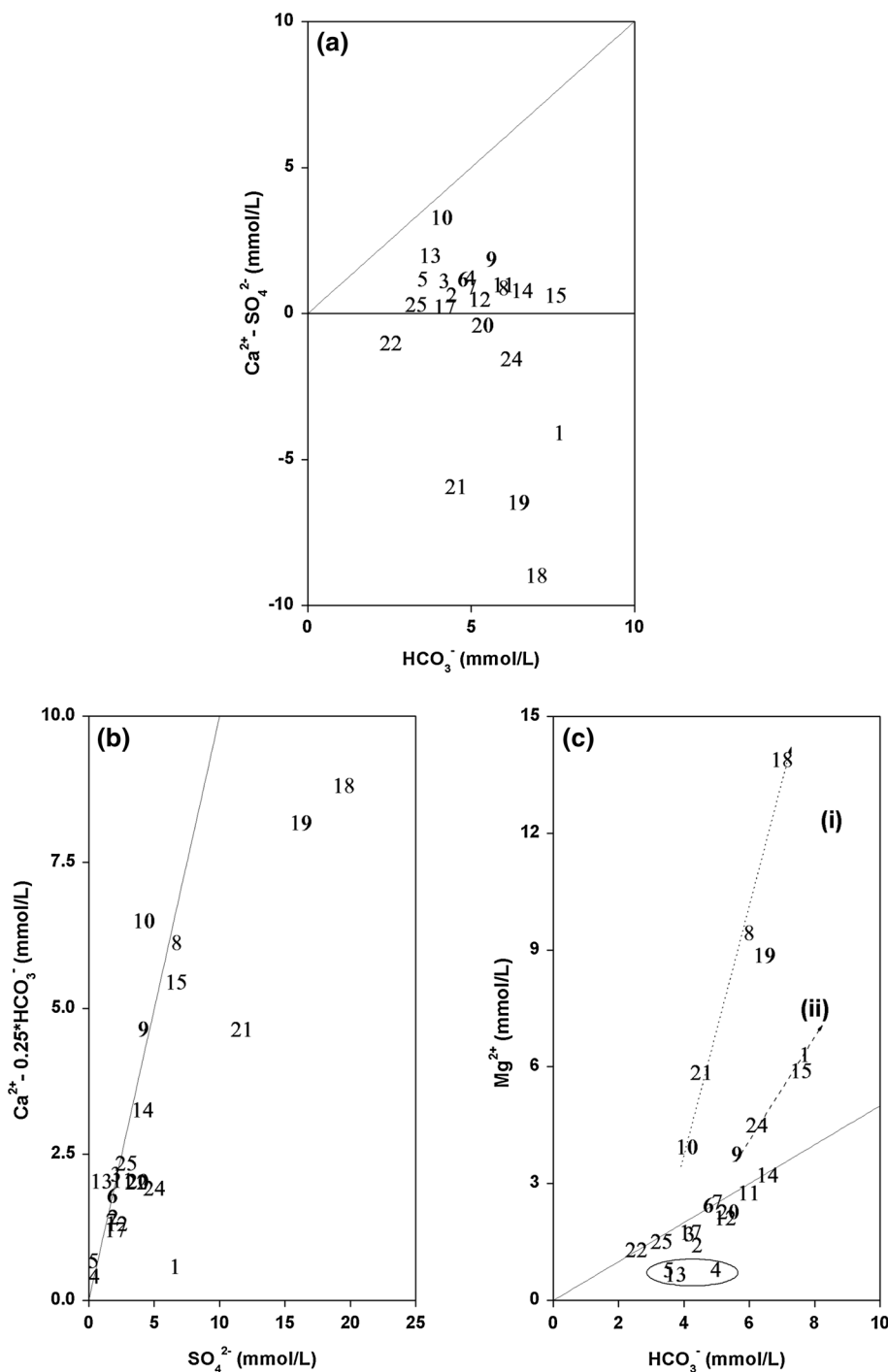
dissolution of high Mg-calcite. Presence of low Mg-calcite precipitates in intergranular pores of some deposits was noticed by Bhatt (2003), who corroborates our finding that high Mg-calcite dissolves incongruently forming low Mg-calcite precipitates. A few samples fall above incongruent dissolution line in two different trends (dotted lines (i) and (ii) in Fig. 8c), which can be attributed to magnesium addition from other sources like ferromagnesium and magnesium silicate minerals in varying amounts. From the

above plots (Fig. 8a–c), it can be concluded that the source of Ca^{2+} and SO_4^{2-} is gypsum and incongruent dissolution of high Mg-calcite is the process controlling Mg^{2+} and HCO_3^- concentrations in groundwater. It can be seen from Fig. 5d and f that HCO_3^- does not show proportionality with chloride concentration, indicating that HCO_3^- concentration is limited by calcite re-precipitation. The dissolution and precipitation processes of carbonate minerals and gypsum are further verified using saturation indices.

Saturation indices (SI) for gypsum and carbonate minerals were determined to investigate the thermodynamic controls on the composition of the water and also to calculate approximately the levels to which the groundwater has equilibrated with these phases within the rock matrix. Saturation index (SI) of groundwater for a particular mineral can be calculated as

$$SI = Log \frac{IAP}{K_{sp}}. \qquad (4)$$

where IAP is the ion activity product and K_{sp} is the mineral solubility product. At saturation, the saturation index equals zero whereas positive and negative values indicate supersaturation and undersaturation, respectively.

Rainwater in equilibrium with atmosphere has a CO_2 partial pressure of $10^{-3.5}$ atm (log pCO_2 −3.5). As the rainwater infiltrates through the soil, CO_2 content increases to a log pCO_2 of −2 (Drever 1997). The log pCO_2 values in groundwaters in the study area range from −0.9 to −2.1. The SI values confirm that most of the groundwaters are unsaturated with respect to gypsum, whereas samples show wide variation in calcite solubility. Plot of $SI_{calcite}$ versus SI_{gypsum} (Fig. 9a) shows that most of the groundwater samples fall close to calcite saturated zones indicating long residence time of the groundwater with the carbonate minerals; however, a few samples from Wagad basin (nos. 20, 21, 22,24 and 25) and Kachchh mainland (no. 2) are unsaturated with respect to calcite. Unsaturation in the case of samples from Wagad basin can be explained by increase in acidic nature of these waters, which can be due to influx of CO_2 from decay of organic matter present in the formation. These samples, except no. 20, are slightly acidic in nature and have high log pCO_2 values −1. Groundwater

samples no. 1, 8 and 18 are super saturated with respect to calcite and are also saline. Supersaturation can be produced by factors such as incongruent dissolution, common ion effect, evaporation, rapid increase in temperature and CO_2 exsolution (Langmuir 1997). Supersaturation with calcite can also be caused by mixing of fresh and saline groundwaters (Langmuir 1971). It is also observed that rates of mixing must be rapid enough to prevent equilibration with groundwater by precipitation of calcite (Langmuir 1971). In the case of sample nos. 8 and 18 shallow zone water samples, it is possible that porous nature of soil allows rapid mixing of precipitation with shallow zone saline water leading to the observed supersaturation with calcite. $SI_{fluorite}$ values of all the water samples fall in fluorite unsaturated zone (Fig. 9b), except in sample no. 8 (F⁻; 5.4 mg/L). This indicates that dissolution of fluorite is a crucial process affecting fluoride concentration in these groundwaters. Majority of the samples fall close to calcite saturation line implying that fluorite dissolution may be driven by precipitation of calcite even though fluorite solubility is low.

Isotope study

Chemical characteristics of groundwater reflect only the dissolved chemical load and this signal can be modified by various physical and chemical processes, whereas environmental isotopes ^2H and ^{18}O are conservative tracers of groundwater as they are part and parcel of water molecule. Deuterium and oxygen-18 have been extensively used in studies such as groundwater recharge, source, origin and movement of groundwater contamination and groundwater salinization (Herczeg and Leaney 2011; Clark and Fritz

Fig. 9 a Plot of saturation index of calcite ($SI_{calcite}$) versus saturation index of gypsum (SI_{gypsum}); b plot of saturation index of calcite ($SI_{calcite}$) versus saturation index of fluorite ($SI_{fluorite}$) of water samples
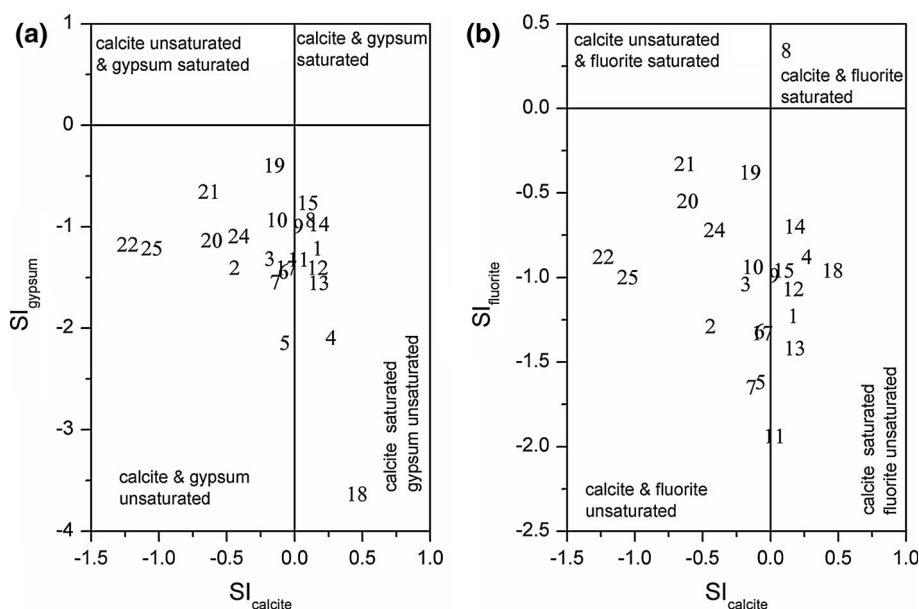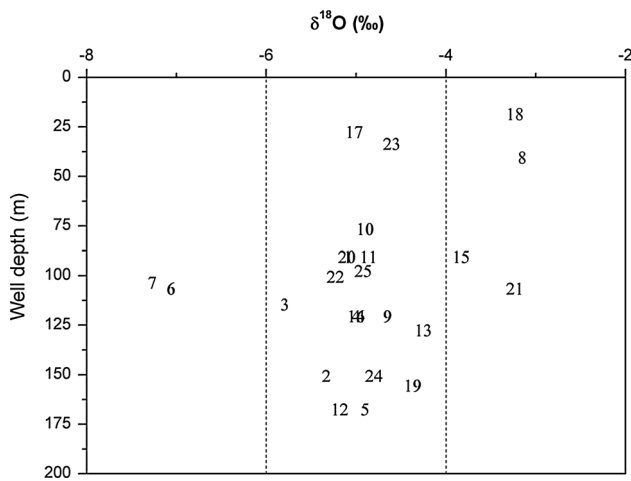
Fig. 10 Plot of $\delta^{18}O$ content of the groundwater samples versus well depth in meters below ground level

1997). The δ^2H and $\delta^{18}O$ composition of the groundwaters are given in Table 5. Groundwater samples from this district show isotopic variation of $\delta^{18}O$ −5.8 to −3.2 ‰ and δ^2H −35.8 to −18.7 ‰. Two samples from Kachchh mainland tapping Tertiary formation show depleted isotopic content ($\delta^{18}O$ −7.2 ‰ and δ^2H −45 and −50 ‰). Depth wise variation of $\delta^{18}O$ in groundwaters is shown in Fig. 10. It can be observed that groundwaters show very narrow distribution of $\delta^{18}O$ content with an average $\delta^{18}O$ value of −4.7 ± 0.7 ‰. Groundwater sample nos. 6 and 7 show depleted isotopic signature, whereas groundwater samples nos. 8, 18 and 21 show enriched isotopic values.

A plot of δ^2H and $\delta^{18}O$ correlations of groundwater data has been presented in Fig. 11a. Global Meteoric Water Line (GMWL: $\delta^2H = 8.17\delta^{18}O + 11.27$) and Indian Meteoric Water Line (IMWL: $\delta^2H = 7.93\delta^{18}O + 9.94$) were also shown in the plot (Rozanski et al. 1993; Kumar et al. 2010). Water samples that are of meteoric origin plot along IMWL with a slope of 7.9, but under certain circumstances the isotopic data of groundwater samples deviate from this line, which include evaporation and mixing (Clark et al. 2000). When water evaporates, lighter isotopes preferentially escapes into vapor phase resulting in enrichment of heavier isotopes in remnant water and the slope of the line varies between 4 and 6 (Clark and Fritz 1997). In the case of mixing between groundwater and other surface or rainwater, the isotope composition of the resultant water falls on the mixing line. Most of the groundwater sample data in this district fall on the IMWL indicating precipitation as the main source of recharge. The inset shows the magnified portion of the plot ($\delta^{18}O$ from −6 to −3 ‰). Best fit line for the isotopic data of the groundwater samples shows a slope of 6.65, indicating slight evaporation. A few groundwater samples (nos. 8, 15, 18 and 21) fall below IMWL (Fig. 11a). Contribution from evaporated shallow zone groundwaters

or seawater mixing could be the reason for the enrichment in isotopic content. Two groundwater samples from Kachchh mainland (nos. 6 and 7) show depleted isotopic composition ($\delta^{18}O$ about −7.5 ‰). This probably indicates that the recharge to these waters might have taken place during cooler climate or flood events (Sukhija et al. 1998), which needs further confirmation by groundwater age dating. Deviation from GMWL is indicated by d-excess parameter (Dansgaard 1964). This parameter is used to signify the kinetic effects associated with the evaporation of water at the surface of the oceans or inland (Clark and Fritz 1997). It is represented by

$$d\text{-excess} = 8 \times \delta^{18}O - \delta^2H. \tag{5}$$

The primary evaporation from the sea surface fixes the d-excess value, which remains unaltered as the air moves across the continents and loses moisture by rainout. However, the d-excess of the air masses are impacted by the secondary process that returns moisture to the air, such as evaporation from an open surface water body (recycling of water). The d-excess in this area ranges from +4.4 to 15 ‰ with an average $\delta^{18}O$ of −4.7 ‰. This indicates that the groundwater has undergone limited modification due to evaporation before its recharge. A similar finding was reported by Gupta et al. (2005).

To identify the sources of brackishness and salinity in groundwater of this district, $\delta^{18}O$ data were plotted against corresponding Cl^- values (Fig. 11b). A theoretical line indicating conservative mixing of seawater and fresh water was also shown in the plot. Seawater as saline end member and sample no. 5 as freshwater end member were used for constructing SW-FW mixing line. Groundwater samples fall in four different groups. Group (a) samples (4, 5, 13, 17 and 23) are groundwater belonging to freshwater category, while Group (b) samples (nos. 6 & 7) show depleted isotopic content and slightly brackish in quality. Group (c) consists of samples from Tertiary and Cretaceous formations of Wagad basin and Kachchh mainland. Brackish quality in these groundwaters can be attributed to acquisition of salts from the formation. It is observed from the δ^2H versus $\delta^{18}O$ plot that these sample data fall on IMWL (Fig. 11a). The samples falling in Group (d) (nos. 8, 15, 18 and 21) show enriched isotopic composition, i.e., brackish to saline in quality. These samples fall on an evaporation line in the plot δ^2H versus $\delta^{18}O$ (Fig. 11a). The brackish to saline quality in these waters could be due to mixing between groundwater and saline water due to evaporation from the shallow zone. From isotope study, it can be understood that the observed brackishness/salinity in groundwater is not due to seawater intrusion, which is in agreement with the major and minor ion trends ("Major ion trends" and "Minor ion trends").
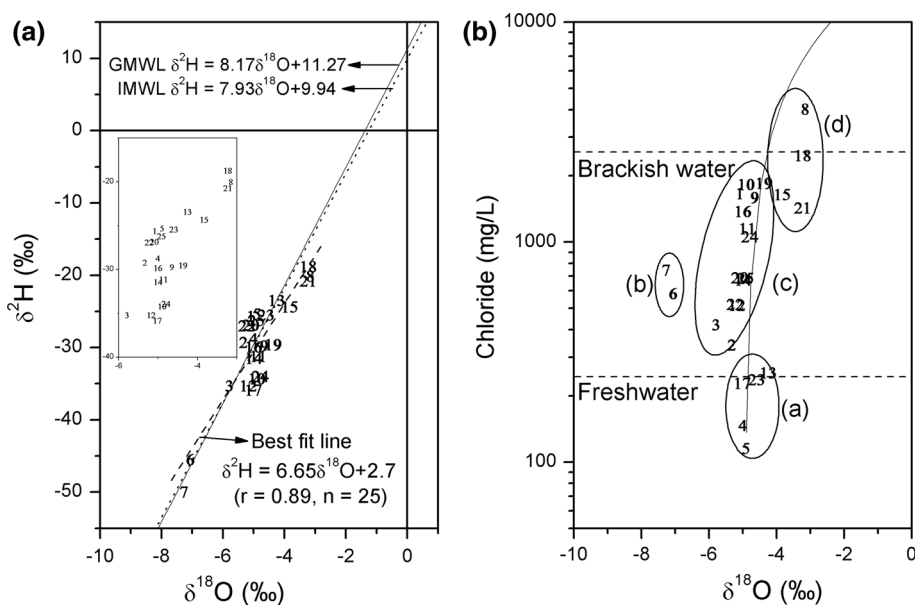
Fig. 11 a Plot of δ^2H versus $\delta^{18}O$ contents (‰ against VSMOW) of groundwater samples. *Solid* and *dashed lines* indicate Global Meteoric Water Line (GMWL, after Rozanski et al. 1993) and Indian Meteoric Water Line (IMWL, after Kumar et al. 2010); *dotted line* is best fit to groundwater sample data with equation shown in the plot; *inset* shows the enlarged portion. **b** Plot of chloride (in mg/L) versus $\delta^{18}O$ (in ‰ against VSMOW) content of water samples. *Solid line*

indicates seawater–freshwater (sw–fw) mixing line, whereas *dotted lines* indicate freshwater (Cl 250 mg/L) and brackish water (Cl 2,500 mg/L) limits. Group (*a*) represents freshwater samples, Group (*b*) represents samples with depleted isotopic content, Group (*c*) comprises samples from Tertiary and Cretaceous formations of Wagad basin and Kachchh mainland, Group (*d*) samples are from Quaternary formation of Kachchh mainland and Wagad basin

From the environmental isotopic inferences, it can be concluded that acquisition of marine salts from the formation is the governing process of salinization of groundwater in this part of Gujarat and not the present day seawater intrusion. Reports suggest that seawater intrusion in coastal Gujarat depends mainly on major ion trends and mixing ratios (Desai et al. 1979). However, these facts need to be reconfirmed with isotope inferences and ionic ratios. Even though isotope studies were carried out by Gupta et al. (2005), isotopic characteristics of groundwater from different zones of this district were not studied and therefore this study fills the gap of the earlier studies.

Summary

Groundwater from major formations of Kachchh district is studied for its quality and geochemical characterization using hydrochemical and isotopic approaches. The groundwater is saline in top Quaternary formation, brackish in Wagad basin and Tertiary formations of Kachchh mainland, and fresh in Cretaceous formation of Kachchh mainland. Deep zone groundwater showed low EC as compared to shallower zone in the Kachchh mainland, while no systematic trend is observed in the case of Wagad basin. This demonstrates that groundwater quality is mainly controlled by lithology of the formation.

Dissolution of marine sediments is found to be the primary reason for brackishness in groundwater, which is further increased by low flushing rates of groundwater especially in the case of Tertiary formations. No inorganic contamination is observed in groundwater as all the measured toxic elements are found to be mostly within permissible limits. Majority of the groundwaters measured indicate TDS values above drinking water desired limits. Similarly, half of the measured samples indicate that the presence of high Na% along with high EC, which causes reduction in osmotic activity of plants and thus interferes with the absorption of water and nutrients from the soil, is therefore unsuitable for irrigation purpose.

Geochemical interpretation suggests incongruent dissolution of high Mg-calcite and re-crystallization of carbonate minerals as the main controlling reactions for the variation of groundwater chemistry. Mg^{2+} increases owing to the incongruent dissolution of high Mg-calcite, while Ca^{2+} remains relatively constant. Sulfate concentration increases as gypsum dissolves and bicarbonate concentration remains relatively constant. Isotope data indicate that the groundwater of this district is of meteoric origin and has undergone limited modification before recharge, which is also supported by *d*-excess content of the groundwater. Major process that controls salinity in groundwater is found to be leaching of marine sediments besides contribution of evaporites from the soil zone. Even though these results

and the derived processes are only valid in the dry season, still it is very likely that with very less and erratic rainfall most of the above said processes are prevalent throughout the year.

Implications for groundwater use

Since the geologic units in this district are composed of marine salty units, there is no suitable unit for groundwater use except from sandstone formation. The Cretaceous sandstone formation of Bhuj is generally without adequate impervious zones forming a favorable formation for water storage. This aquifer can be regarded as a single aquifer and it is sustained by direct percolation of precipitation. Groundwater quality is brackish to saline in shallow zone, while it is fresh in deeper zones indicating contribution of salts from shallow zones that are formed due to evaporation process; hence, large-scale groundwater recharge measures in this formation can be practiced to dilute the salinity and also mitigate the growing groundwater crises. With these measures, groundwater suitability for irrigation can be improved up on by reducing SAR, Na% and other critical parameters. Recharge experiments, in large scale, are in practice in Saurashtra region of Gujarat as reported by Gupta and Deshpande (2004). Inter-basin transfer of water as proposed by National Water Development Agency can also be of great relief to the present water scarcity in this district (TF-IRL 2003) considering the scanty and irregular rainfall.

References

Baskaran M, Deshpande SV, Rajaguru SN, Somayajulu BLK (1989) Geochronology of miliolite rocks of Kutch, Western India. J Geol Soc India 33:588–593

Bhatt N (2003) The late quaternary bioclastic carbonate deposits of Saurashtra and Kachchh, Gujarat, Western India: a review. Proc Indian Nat Sci Acad 69:137–150

BIS (2004) Indian standard drinking water—specifications second revision of IS 10500

Biswas SK (1987) Regional tectonic framework, structure and evolution of the western marginal basins of India. Tecnophysics 135:307–327

CGWB (2009) http://cgwb.gov.in/documents/gec97.pdf

Clark ID, Fritz P (1997) Environmental isotopes in hydrogeology. Lewis Publishers, New York

Clark ID, Douglas M, Raven K, Bottomley D (2000) Recharge and preservation of Laurentide glacial melt water in Canadian Shield. Ground Water 38:735–742

Dansgaard W (1964) Stable isotopes in precipitation. Tellus 16:436–468

Davis JH (1977) Genesis of the southeast Missouri lead deposits. Econ Geol 72:443–450

Davis SN, Wiest De (1996) Hydrogeology. Wiley, New York, p 46

Desai BI, Gupta SK, Shah MV, Sharma SC (1979) Hydrochemical evidence of seawater intrusion along the Mangrol-Chorwad coast of Saurashthra, Gujarat. Hydrol Scien Bull 24:71–82

Domenico PA, Schwartz FW (1990) Physical and chemical hydrogeology. Wiley, New York, pp 410–420

Doneen LD (1948) The quality of irrigation water, vol 4. California Agriculture Department, USA, pp 6–14

Drever JI (1997) The geochemistry of natural waters, surface and groundwater environments, 3rd edn. Prentice-Hall Publishers, USA

Durfor CN, Becker E (1964) Public water supplies of the 100 largest cities in the United States, water supply paper No. 1812, pp 343–346

Edmunds WM (2009) Geochemistry's vital contribution to solving water resource problems. Appl Geochem 24:1058–1073

Edmunds WM, Cook JM, Darling WG, Kinniburgh DG, Miles DL (1987) Baseline geochemical conditions in the Chalk aquifer, Berkshire, U.K.; a basis for groundwater quality management. App Geochem 2:251–274

Elliot T, Chadha DS, Younger PL (1998) The regional hydrochemistry and water quality in the East Yorkshire chalk aquifer, U.K.. In: Proceedings of the Yorkshire Geological Society

Glynn PD, Plummer LN (2005) Geochemistry and the understanding of ground-water systems. Hydrgeol J 13:263–287

Gupta SK, Deshpande RD (2004) Water for India in 2050: first-order assessment of available options. Curr Sci 86:1216–1224

Gupta SK, Deshpande RD, Bhattacharya SK, Jani RA (2005) Groundwater $\delta^{18}O$ and δ^2H from central Indian peninsula: influence of the Arabian Sea and Bay of Bengal braches of the summer monsoon. J Hydrol 303:38–55

Hanshaw BB, Back W (1979) Major geochemical processes in the evolution of carbonate-aquifer systems. J Hydrol 43:287–312

Herczeg AL, Leaney FW (2011) Review: environmental tracers in arid-zone hydrology. Hydrogeol J 19:17–29

Hitchon Brian, Perkins EH, Gunter WD (1999) Introduction to ground water geochemistry. Geoscience Publishing Ltd, Canada

IWMI-TATA (2005) Fourth annual partners research meet, 24–26 Feb 2005, Indira Hirway, pp 1–46

Karanth KR (1987) Groundwater assessment, development and management. Tata-McGraw-Hill, New Delhi

Karanth RV (2006) Structure and tectonics of Kachchh region of western India: an appraisal http://www.gisdevelopment.net/application/natural_hazards/earthquakes/nheq0004pf.htm

Khadkikar AS, Mathew G, Malik JN, Gundu Rao TK, Chowgoankar M, Merh SS (1999) The influence of the Southwest Indian monsoon on continental deposition over the past 130 kyrs, Gujarat, western India. Terra Nova 11:272–277

Krishnan MS (1949) Geology of India and Burma, geological survey of India. The Madras Law Journal Press, Mylapore, Chennai

Kumar B, Rai SP, Kumar US, Verma SK, Garg P, Kumar SVV, Jaiswal R, Purendra BK, Kumar SR, Pande NG (2010) Isotopic characteristics of Indian precipitation. WRR 46(12). doi:10.1029/2009WR008532

Langmuir D (1971) The geochemistry of some carbonate groundwaters in central Pennsylvania. Geochim Cosmochim Acta 35:1023–1045

Langmuir D (1997) Aqueous environmental geochemistry. Prentice-Hal, New Jersy

Lyès Ferroukhi (1996) Survival against the odds through creativity. International Rural, Development Centre (IRDC), Swedish, University of Agricultural Sciences (SLU), pp 34–39

Maurya DM, Thakkar MG, Chamyal LS (2003) Implications of transverse fault system on tectonic evolution of mainland Kachchh, Western India. Curr Sci 85:661–667

Mercado A (1985) The use of hydrochemical patterns in carbonate sand and sandstone aquifers to identify intrusion and flushing of saline water. Ground Water 23:635–645

Merh SS (1993) Neogene-Quaternary sequence in Gujarat: a review. J Geol Soc India 41:259–276

Merh SS (1995) Geology of Gujarat. Published by Geological Survey of India

Pande D, Kulkarni KM, Muralidharan R, Panchal PK, Rao SS, Ravi Kaul (1991) Hydrogeochemical exploration for Uranium—a case study of Kutch Basin, Gujarat, India. In: Proceeding of International symposium on applied geochemistry, Hyderabad, pp 61–66

Parag SS (2002) Tectono-structural attributes of central Kachchh mainland with special emphasis on active tectonics and palaeoseismicity. J Geol Soc India 60:114–116

Plummer LN, Prestemon EC, Parkhurst DL (1994) An interactive code (NETPATH) for modeling Net geochemical Reactions along a flow path (ver. 2.0). U.S. Geological Survey, Water-Resources Investigations Report 94-4169

Ragunath HM (1987) Groundwater, 2nd edn. Wiley Eastern Ltd, New Delhi, p 563

Ramakrishna (1998) Groundwater handbook, India

Richards LA (1954) Diagnosis and improvement of saline and alkali soils. US Department of Agriculture Agriculture Hand book 60, Washington

Rittenhouse G, Fulton RB, Grabowski RJ, Bernard JL (1969) Minor elements in oil field waters. Chem Geol 4:184–209

Rozanski K, Araguas-Araguas L, Gofiantini R (1993) Isotope patterns in modern global precipitation. In: Continental Isotope Indicators of Climate, American Geophysical Union Monograph

Singh YD, Vijaya Kumar V, Wesley SSF, Dixit AM (1996) Process of desertification in Kachchh and Banaskantha Districts of Gujarat, India. Gujarat Institute of Desert Ecology, Bhuj (Kachchh). http://www.gec.gov.in

Sukhija BS, Reddy DV, Nagabhushanam (1998) Isotopic fingerprint of palaeoclimates during the last 30,000 years in deep confined groundwaters of Southern India. Quat Res 50:252–260

Taylor GC, Pathak BD (1960) Geology and groundwater resources of the Anjar-Khedoi region, eastern Kutch, India, India Geology Survey, Ser. B, Bull. 9, p 339

TF-IRL (2003) Inter basin water transfer proposals. Task force on inter-linking of Rivers, Ministry of water resources, Government of India, New Delhi, p 27

Thakkar MG, Maurya DM, Raj Rachna, Chamyal LS (1999) Quaternary tectonic history and terrain evolution of the area Around Bhuj, Mainland Kachchh, Western India. J Geol Soc India 53:601–610

Tijani MN (1994) Hydrochemical assessment of groundwater in Moro area, Kwara State, Nigeria. Environ Geol 24:194–202

Trivedy RK, Goel PK (1984) Chemical and biological methods for water pollution studies. Environmental Publication, Karad

Vengosh A, Arthur J, Spivack Yohanan Artzi, Ayalon Avner (1999) Geochemical and boron, strontium, and oxygen isotopic constraints on the origin of the salinity in groundwater from the Mediterranean coast of Israel. WRR 35:1877–1894

Wadia DN (1973) Geology of India. Tata-Mc Graw-Hill Publishing Company, pp 248–251, 276–280

WHO (2008) Guidelines for drinking-water quality, 3rd Edition, vol 1 Recommendations Fluorides and oral health, World Health Organization, Technical Report. Series No. 846, Geneva

Wilcox LV (1955) The quality of water for irrigation use. U.S. Department of Agriculture, Tech, Bull, 962, Washington, pp 1–40